Electrochimica Acta 55 (2009) 451–457

Contents lists available at ScienceDirect

Electrochimica Acta

journal homepage: www.elsevier.com/locate/electacta

Alloy formation during the electrochemical growth of a Ag–Cd ultrathin film on Au(1 1 1)

M.C. del Barrio, S.G. García [1], D.R. Salinas [*,1]

Instituto de Ingeniería Electroquímica y Corrosión (INIEC), Departamento de Ingeniería Química, Universidad Nacional del Sur, Avda. Alem 1253, 8000 Bahía Blanca, Argentina

ARTICLE INFO

Article history:
Received 5 May 2009
Received in revised form 19 August 2009
Accepted 20 August 2009
Available online 27 August 2009

Keywords:
Au(1 1 1)–Ag–Cd system
Thin films
Surface alloys
In situ STM
UPD–OPD

ABSTRACT

The electrodeposition of a Ag/Cd ultrathin film on a Au(1 1 1) surface and the formation of a surface alloy during this process have been studied using classical electrochemical techniques and *in situ* Scanning Tunneling Microscopy (STM). The films were obtained from separate electrolytes containing Ag^+ or Cd^{2+} ions and from a multicomponent solution containing both ions. First, the polarization conditions were adjusted in order to form a Ag film by overpotential deposition. Afterwards, a Cd monolayer was formed onto this Au(1 1 1)/Ag modified surface by underpotential deposition. The voltammetric behavior of the Cd UPD and the *in situ* STM images indicated that the ultrathin Ag films were uniformly deposited and epitaxially oriented with respect to the Au(1 1 1) surface. Long time polarization experiments showed that a significant Ag–Cd surface alloying accompanied the formation of the Cd monolayer on the Au(1 1 1)/Ag modified surface, independent of the Ag film thickness. In the case of an extremely thin Ag layer (1 Ag ML) the STM images and long time polarization experiments revealed a solid state diffusion process of Cd, Ag, and Au atoms which can be responsible for the formation of different Ag–Cd or Au–Ag–Cd alloy phases.

1. Introduction

The electrochemical formation of ultrathin metallic films formed on foreign substrates (metals, superconductors and semiconductors) has received considerable attention from both fundamental and applied viewpoints [1–7]. This type of ultrathin films can be electrochemically obtained by underpotential deposition (UPD) or overpotential deposition (OPD), since the coverage of metal deposits from submonolayers up to several monolayers can be well adjusted through charge measurements. The UPD process is referred as the electrodeposition of a metal (Me) on a foreign substrate (S) at potentials more positive than the Nernst equilibrium potential of the three-dimensional (3D) metal bulk phase (E_{3DMe}). In contrast, the OPD denotes the electrodeposition at potentials more negative than the E_{3DMe} and different deposition mechanisms can be operative [1,7]. While this way of achieving well-controlled ultrathin layers is well known since long time ago, the atomistic study and the nanometric control together with the analysis linking the substrate properties and the adsorbate characteristics, have been enhanced using SPM techniques [8,9], improving the development of new catalysts and surface alloys.

Metallic heterostructures formed by more than one component onto a given substrate play an important role in modern electrochemistry, mainly in the preparative aspects of electrochemical nanotechnology, by their important application in the development of new materials with unconventional properties. This type of heterostructures can be also obtained by electrodeposition, but only few studies have been reported using the single metals UPD [10–17]. In some cases, it is possible to obtain a "sandwich" structure constituted by a succession of metallic ultrathin films and/or surface alloys [12,13,18–21], if the conductive substrate is conveniently polarized in a multicomponent electrolyte, i.e. an electrolyte containing more than one metallic cation. These structures can be electrochemically obtained in the corresponding UPD or OPD ranges, depending on the equilibrium potentials of the deposited metals, their interaction energies and the crystallographic misfit between the adatom and the substrate lattice [3], as well as the polarization conditions.

In a previous paper [22] it was demonstrated that it is possible to obtain an ultrathin Ag–Cd bimetallic layer with epitaxial arrangement in the system Au(1 1 1)/Ag^+, Cd^{2+}, SO_4^{2-}, because both Au(1 1 1)/Ag^+ and Ag(1 1 1)/Cd^{2+} systems show underpotential deposition with the corresponding UPD regions sufficiently separated. Moreover, a layer-by-layer mechanism operates in the system Au(1 1 1)/Ag^+ in the OPD range and the metal–substrate crystallographic misfit is very low ($d_{0,Au}$ = 0.2884 nm, $d_{0,Ag}$ = 0.2889 nm, $d_{0,Cd}$ = 0.2978 nm) in both systems, opening an excellent possibility to study the preparation

* Corresponding author. Tel.: +54 291 4595182; fax: +54 291 4595182.
E-mail address: dsalinas@uns.edu.ar (D.R. Salinas).
[1] ISE member.

0013-4686/$ – see front matter © 2009 Elsevier Ltd. All rights reserved.
doi:10.1016/j.electacta.2009.08.032

of sandwich-structure metal films [3,12]. Nevertheless, considering the significant Ag–Cd and Au–Cd surface alloying process reported during the UPD in the systems Ag(1 1 1)/Cd^{2+} [23] and Au(1 1 1)/Cd^{2+} [24,25], the formation of a Au–Ag–Cd alloy should be considered. The aim of the present paper is the study of this surface alloying process using conventional electrochemical techniques and *in situ* STM. The Ag/Cd ultrathin film was formed onto the Au(1 1 1) substrate from separate electrolytes containing Ag^+ or Cd^{2+} ions, and from a multicomponent solution containing both ions.

2. Experimental

The experiments were carried out using a Au(1 1 1) single crystal electrode, with a diameter of 4 mm, as a working electrode. The substrate surface was first mechanically polished with diamond paste of decreasing grain size down to 0.25 μm and subsequently electrochemically polished in a cyanide bath according to a standard procedure [26].

The electrolyte solutions used throughout the study were:

1 mM $CdSO_4$ + 5 mM H_2SO_4 + 0.1 M Na_2SO_4,

*y*mM Ag_2SO_4 + 5 mM H_2SO_4 + 0.1 M Na_2SO_4, with $y = 0.015$ and 5,

1 mM $CdSO_4$ + 0.015 mM Ag_2SO_4 + 5 mM H_2SO_4 + 0.1 M Na_2SO_4.

These solutions were prepared from suprapure chemicals (Merck, Darmstadt) and fourfold quartz-distilled water, and deareated by nitrogen bubbling prior to each experiment.

Classical electrochemical studies were performed in standard three-electrode electrochemical cells. The counter-electrode was a platinum sheet (1 cm^2) and the reference electrode was a $Hg/Hg_2SO_4/K_2SO_4$ saturated electrode (SSE), mounted inside a Luggin capillary. The actual electrode potential, E, is referred to the SSE, whereas the underpotential, ΔE_{3DMe}, or the overpotential, η_{3DMe}, are related to the corresponding Nernst equilibrium potential of the 3D metal phase (E_{3DMe}) by $\Delta E_{3DMe} = E - E_{3DMe} > 0$, or $\eta_{3DMe} = E - E_{3DMe} < 0$, respectively. The measurements were carried out with a potentiostat–galvanostat EG&G Princeton Applied Research Model 273A.

A Nanoscope III standard equipment (Digital Instruments, Santa Barbara, CA, USA) was used for the *in situ* STM studies, employing Apiezon insulated Pt–Ir tips (Veeco, USA). A Pt wire was used as counter-electrode and a Au wire as quasi-reference electrode. The potentials of the gold substrate and the STM tip were controlled independently by a Nanoscope III-bipotentiostat optimized for the STM set-up used. The tip potential was held constant at a value of minimum faradaic current and the tip current varied in the range $2 \leq I_{tun}\,(nA) \leq 20$. The experimental set-up for the *in situ* STM technique has been checked by cyclic voltammetric measurements and the results were identical to those obtained in the conventional electrochemical cell.

3. Results and discussion

Fig. 1 shows typical cyclic voltammograms, already published, for the systems Au(1 1 1)/Ag^+, SO_4^{2-} [27], Ag(1 1 1)/Cd^{2+}, SO_4^{2-} [23], and Au(1 1 1)/Cd^{2+}, SO_4^{2-} [24] in order to illustrate the UPD–OPD regions of the binary systems. These voltammograms were described in a previous work [22]. The cyclic voltammogram for Ag UPD on Au(1 1 1) shows two characteristic sorption peaks at $\Delta E_{3DAg} = 600 \pm 120$ mV and at underpotentials close to the E_{3DAg} (Fig. 1a). Buess-Herman et al. [28] have indicated that potential cycling of Au(1 1 1) in the Ag^+ containing solution produces surface disordering associated with a place exchange mechanism, resulting in the formation of a Ag–Au surface alloy. This condition affects the potentials and intensity of the UPD peaks, as well

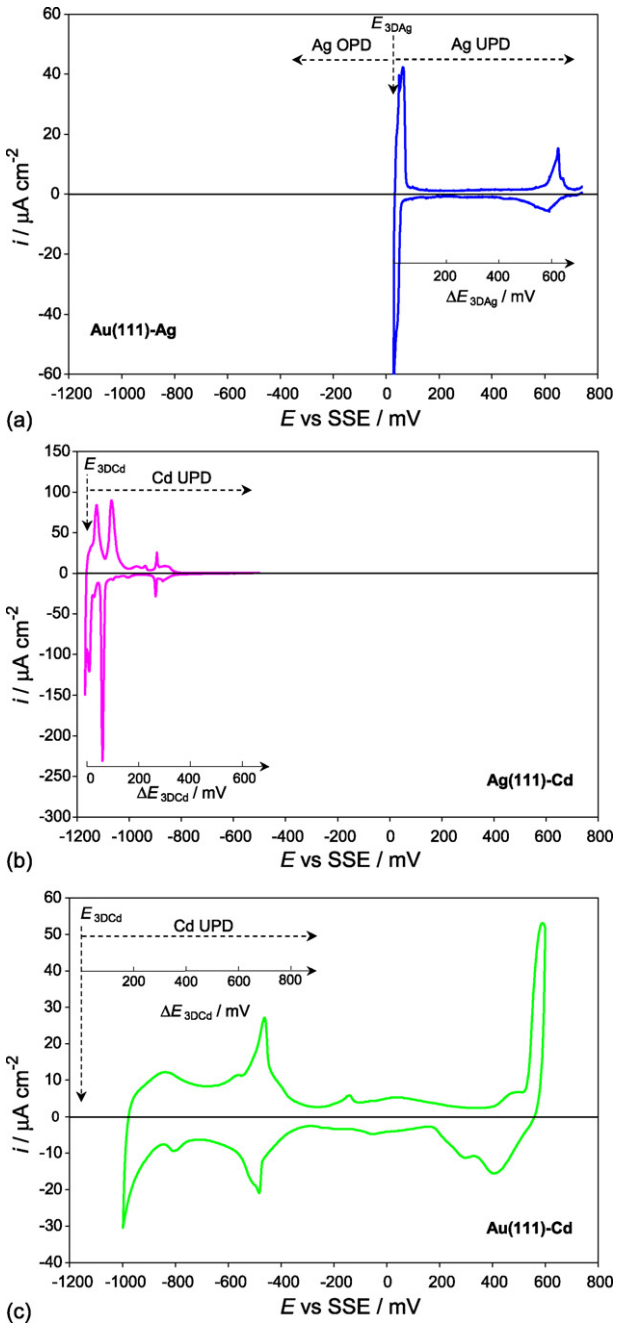

Fig. 1. Cyclic voltammograms for the binary systems: (a) Au(1 1 1)/5 mM Ag_2SO_4 + 0.1 M H_2SO_4, $|dE/dt| = 7\,mV\,s^{-1}$, (b) Ag(1 1 1)/1 mM $CdSO_4$ + 5 mM H_2SO_4 + 0.1 M Na_2SO_4, $|dE/dt| = 10\,mV\,s^{-1}$, (c) Au(1 1 1)/1 mM $CdSO_4$ + 5 mM H_2SO_4 + 0.1 M Na_2SO_4, $|dE/dt| = 50\,mV\,s^{-1}$. $T = 298$ K.

as the OPD process, providing sites for nucleation and growth of bulk silver microcrystallites. In the absence of such defects and due to the negligible metal/substrate crystallographic misfit, Kolb et al. [29] reported a layer-by-layer growth mode in the OPD range, up to at least 10 Ag monolayers (10 Ag ML), with a subsequent multilayer growth mode. For the system Ag(1 1 1)/Cd^{2+}, SO_4^{2-}, the cyclic voltammogram (Fig. 1b) displays four Cd UPD peaks in the UPD range $0 \leq \Delta E_{3DCd}\,(mV) \leq 400$. At long polarization times, the condensed Cd ML formed at lower ΔE_{3DCd} undergoes structural changes involving a place exchange process between Cd atoms and surface Ag atoms. At $\Delta E_{3DCd} < 50$ mV a second Cd ML and a significant Ag–Cd surface alloying take place. Finally, the cyclic voltammogram for the Cd UPD on Au(1 1 1) exhibits three

adsorption/desorption current peak pairs in the underpotential range $0 \leq \Delta E_{3DCd}\,(mV) \leq 800$ (Fig. 1c). Current–potential desorption spectra recorded after long polarization times, as well as STM studies demonstrated the formation of 3D Au–Cd alloy phases at $\Delta E_{3DCd} \leq 70$ mV in this binary system [24,30].

Taking into account the stability ranges for the UPD and OPD phases of the binary systems shown in Fig. 1, it is possible to form some Ag ML on the Au(1 1 1) substrate by OPD, followed by 1–2 Cd ML on this Au(1 1 1)/Ag modified surface, producing a Au–Ag–Cd heterostructure [22]. This sequential deposition of Ag and Cd could be achieved from separate electrolytes, containing only Ag^+ or Cd^{2+} ions, as well as from a multicomponent solution containing both ions.

3.1. Au–Ag–Cd heterostructure formed from electrolytes containing only Ag^+ or Cd^{2+} ions

The Ag–Cd bilayer was initially formed onto the Au(1 1 1) surface by sequential deposition from separate electrolytes containing Ag^+ or Cd^{2+} ions. The Ag film was obtained under potentiostatic conditions, in the solution 0.015 mM Ag_2SO_4 + 5 mM H_2SO_4 + 0.1 M Na_2SO_4. The electrode was polarized in the Ag OPD region, at $E = -294$ mV ($\eta_{3DAg} = -170$ mV) during different deposition times, t_d. Under these conditions the Ag electrodeposition process occurred under diffusion control with a relatively low deposition rate, allowing a relatively easy control of the Ag coverage through the deposition time. Besides, under potentiostatic condition the formation of a Au–Ag surface alloy by a place exchange mechanism can be disregarded [28]. The number of Ag ML was estimated from the charge recorded during the corresponding i-t_d transient. The deposition time ranged from $t_d = 16$ h up to $t_d = 1800$ s, in order to obtain deposits with an equivalent charge from $x \approx 480$ Ag ML up to $x \approx 1$–2 Ag ML. Then, the Au(1 1 1)/x Ag ML modified electrode was transferred to an electrochemical cell with the solution containing only Cd^{2+} ions. The procedure of Laibinis et al. [16] was followed in order to maintain the Ag coverage constant: the modified electrode was removed from the first cell under potential control, immediately washed with ethanol, dried in a flow of N_2 and placed in the second cell also under potential control.

Fig. 2 shows the voltammetric response of a Au(1 1 1)/480 Ag ML modified surface in this solution. The voltammogram is relatively similar to that obtained with a Ag(1 1 1) single crystal electrode. This behavior suggests that the Au(1 1 1) was completely screened by a 3D Ag film homogeneously distributed onto the surface and epitaxially oriented with respect to the substrate. The morphology of this Ag film was studied by *in situ* STM in the Cd^{2+} ions containing electrolyte, at a potential value where no Cd adsorption/deposition takes place. The Ag deposit was constituted by atomically flat terraces separated by monatomic steps (Fig. 3), which is in accordance with the results reported by Kolb et al. [29]. These authors concluded that a layer-by-layer growth mode is operative during the first stage of the Ag deposition, followed by a multilayer growth mode.

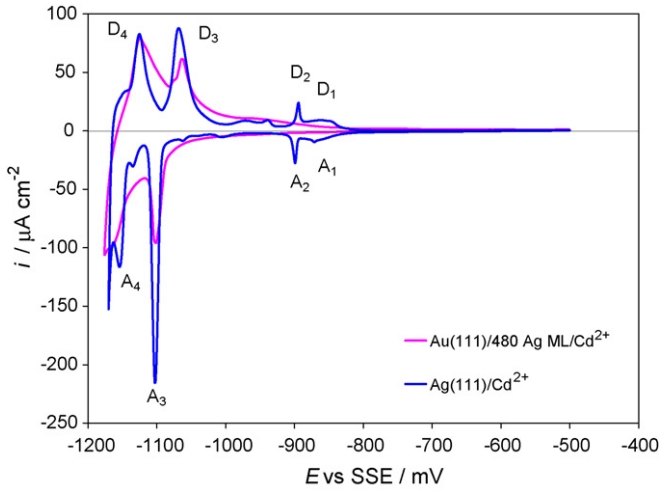

Fig. 2. Cyclic voltammograms for the systems Ag(1 1 1)/Cd^{2+}, SO_4^{2-} and Au(1 1 1)/480 Ag ML/Cd^{2+}, SO_4^{2-}. Electrolyte: 1 mM $CdSO_4$ + 5 mM H_2SO_4 + 0.1 M Na_2SO_4. $T = 298$ K, $|dE/dt| = 10$ mV s^{-1}.

The thickness of the Ag deposit on the Au(1 1 1) surface was progressively decreased, in order to know how many Ag ML are necessary to obtain the voltammetric response of a Ag(1 1 1) electrode. Fig. 4 shows the cyclic voltammograms for the systems Au(1 1 1)/x Ag ML/Cd^{2+}, SO_4^{2-}, where x is the number of Ag ML deposited onto Au(1 1 1), calculated from equivalent charge measurements. From this result it is possible to observe that, until 15 Ag ML, the potentials of the A_3/D_3 and A_4/D_4 Cd UPD peaks, are practically unchanged irrespective of the number of the Ag ML onto Au(1 1 1). Lower thickness produced a displacement of the A_3 and A_4 peaks towards more negative potentials and they are still recorded when only 2 Ag ML are present onto the Au(1 1 1) surface. Moreover, the Cd UPD peaks onto the Au(1 1 1) surface are absent in the potential region $-1150 \leq E\,(mV) \leq -300$ ($0 \leq \Delta E_{3DCd}\,(mV) \leq 850$) (cf. Fig. 1c). These results are evidences of the complete screening of the Au(1 1 1) surface by a Ag layer, on which a monolayer of Cd could be deposited at the Cd^{2+}/Cd^0 equilibrium potential.

Considering the important surface alloy process reported during the Cd UPD onto both surfaces, Au(1 1 1) [24,30] and Ag(1 1 1) [23], long time polarization experiments were carried out at low ΔE_{3DCd}, in order to evaluate the influence of the ultrathin Ag film thickness on this process. The anodic stripping curves obtained with a Au(1 1 1)/300 Ag ML modified substrate after different polarization times, t_p, at $E = -1140$ mV ($\Delta E_{3DCd} = 10$ mV) are shown in Fig. 5a. For a high number of Ag ML onto the Au(1 1 1) surface, the

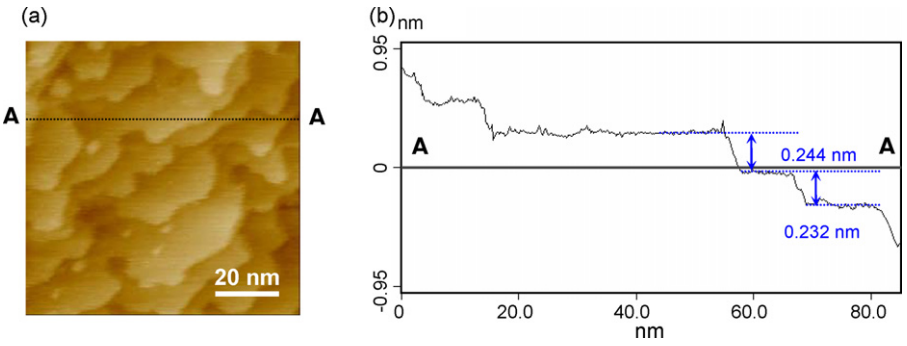

Fig. 3. (a) *In situ* STM image, obtained in 1 mM $CdSO_4$ + 5 mM H_2SO_4 + 0.1 M Na_2SO_4, of the Au(1 1 1) surface topography modified with 480 Ag ML, at $E = -720$ mV ($\Delta E_{3DCd} = 430$ mV). (b) Corresponding cross-section along the line A–A indicating monatomic steps.

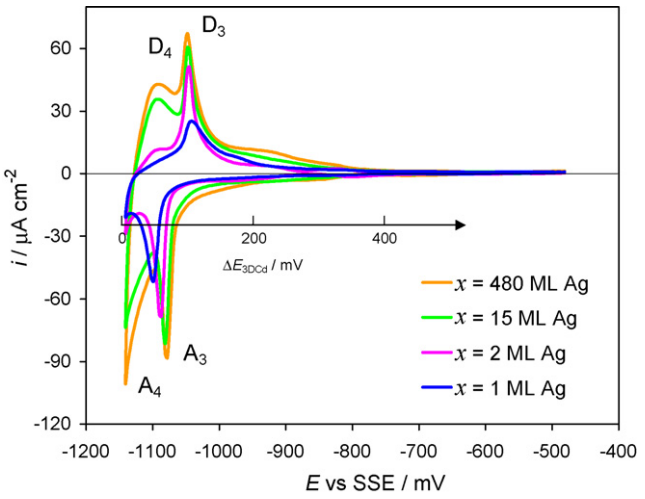

Fig. 4. Cyclic voltammograms for the system Au(1 1 1)/*x* Ag ML/Cd^{2+}, SO_4^{2-}, with *x*: number of Ag ML. Electrolyte: 1 mM $CdSO_4$ + 5 mM H_2SO_4 + 0.1 M Na_2SO_4. T = 298 K, $|dE/dt|$ = 10 mV s^{-1}.

desorption spectra shows that the peak D_4 does not remain stable and its height increases with t_p, and simultaneously, a slight displacement towards highest underpotential values is observed. Moreover, another desorption peak, D', appears at $E = -940$ mV ($\Delta E_{3DCd} = 210$ mV). This peak is related to a Ag–Cd surface alloy dissolution as was reported for the binary system Ag(1 1 1)/Cd [23]. The inset of Fig. 5a shows that the stripping charge density, Δq, increases significantly with t_p, exceeding that required for the deposition of a closed-packed Cd ML ($\Delta q_{CdML} = 444\ \mu C\ cm^{-2}$ assuming the formation of a (1×1) structure). The $\Delta q - t_p^{1/2}$ linear dependence showed in Fig. 5a has been previously discussed [23,31,32] in terms of a semiinfinite-linear diffusion model assuming non-stationary mutual diffusion of Ag and Cd in the Ag/Ag–Cd/Cd^{2+} system. It has been suggested that the alloy formation process proceeds by a movement of Ag atoms through a highly distorted Ag–Cd alloy layer and simultaneous Cd deposition at the Ag–Cd/Cd^{2+} interface, and the kinetic results were fitted [22] with the diffusion model proposed by Vidu and Hara [32]. This model considers that the Ag–Cd alloy layer consists of two regions characterized by different diffusion properties: a thin surface alloy layer with an effective diffusion coefficient D_1, and an inner region characterized by a lower diffusion coefficient D_2. Following the procedure described in Refs. [32,23] these diffusion coefficients were estimated for the Au(1 1 1)/300 Ag ML/Cd system from the $\Delta q - t_p^{1/2}$ linear dependence showed in Fig. 5a, resulting $D_1 = 1.2 \times 10^{-16}$ cm^2/s and $D_2 = 3.14 \times 10^{-18}$ cm^2/s. These values are in good agreement with those reported for the system Ag(1 1 1)/Cd [23].

The behavior described above was also observed when the number of Ag ML onto the Au(1 1 1) substrate is decreased. However, the charges involved in the anodic stripping peaks D_3 and D_4 are lower in the presence of only 1–2 Ag ML (Fig. 5b), the curves are distorted and an additional peak D'' is recorded at long polarization times ($t_p > 600$ s). Thus, two different $\Delta q - t_p^{1/2}$ linear dependences are observed for short and long polarization times (inset of Fig. 5b). The behavior at short polarization times can be attributed to the occurrence of place exchange processes leading to the formation of a thin Ag–Cd surface alloy film on the substrate surface. After this process, the formation of a Au–Ag–Cd alloy starts into the bulk of the Au substrate which is responsible for the appearance of the peak D'' and the fast increase of the stripping charge. The diffusion coefficient D_3 for this last process could be estimated considering the equation $\Delta q = \theta 2Fc_0(D_3/\pi)^{1/2} t_p^{1/2}$ [3] where θ is the Cd coverage at a given potential, c_0 is the Cd concentration at the electrode/electrolyte interface and F is the Faraday constant. Assuming the formation of a complete close packed Cd monolayer results $c_0 = 0.0735$ mol/cm^3 and a value $D_3 = 1.12 \times 10^{-16}$ cm^2/s is obtained, which is close to that observed in the system Au(1 1 1)/Cd [24].

3.2. Au–Ag–Cd heterostructure formed from a solution containing both Ag^+ and Cd^{2+} ions

As was demonstrated in a previous paper [22], it is possible to prepare an ultrathin Ag–Cd bimetallic layer on Au(1 1 1) by sequential electrodeposition from a solution containing both Ag^+ and Cd^{2+} ions. The resulting film is epitaxially oriented with respect to the substrate. However, considering the results presented in the previous section, it is necessary to analyze the formation of a Ag–Cd alloy in the course of this process. The polarization routine indicated in the inset of Fig. 6 (routine 1) was applied on the Au(1 1 1) substrate in order to obtain a bimetallic Ag–Cd layer from the multicomponent solution 0.015 mM Ag_2SO_4 + 1 mM $CdSO_4$ + 5 mM H_2SO_4 + 0.1 M Na_2SO_4 [22]. Initially, the Ag deposition was produced on the Au(1 1 1) surface by polarizing the substrate at $E_{start} = -200$ mV during $t_d = 2400$ s. This potential value is located in the corresponding OPD range of the Ag^+/Ag^0 system ($\eta_{3DAg} = -75$ mV), and it is positive enough to prevent Cd adsorption ($\Delta E_{3DCd} = 970$ mV) [24,29]. After that, the Au(1 1 1)/Ag modified substrate was scanned towards more negative potentials up to $E = -1150$ mV, in order to form a Cd ML. It is important to note that the concentration of the less noble species (Cd^{2+} ions) is sufficiently higher than the more noble ones (Ag^+ ions) so as to produce

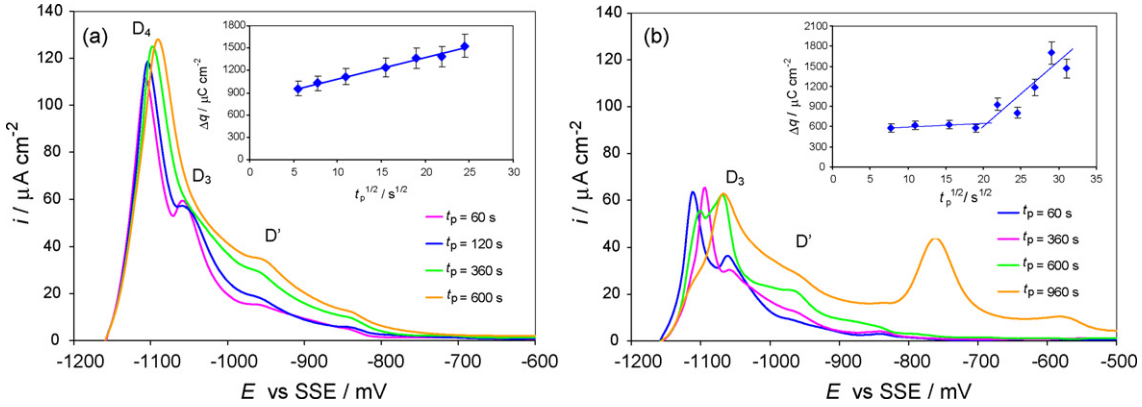

Fig. 5. Anodic stripping curves obtained after different polarization times, t_p, at $E = -1140$ mV, T = 298 K, $|dE/dt|$ = 10 mV s^{-1}. The inset is the corresponding stripping charge density, Δq, as a function of $t_p^{1/2}$. System: Au(1 1 1)/*x* Ag ML/1 mM $CdSO_4$ + 5 mM H_2SO_4 + 0.1 M Na_2SO_4, with *x* = (a) 300, (b) 2. Error bars were estimated for a confidence interval of 90%.

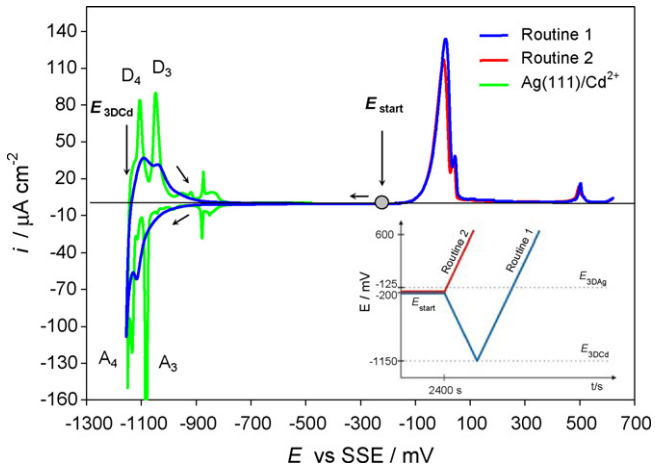

Fig. 6. Voltammetric adsorption/desorption behavior of the system Au(1 1 1)/0.015 mM Ag_2SO_4 + 1 mM $CdSO_4$ + 5 mM H_2SO_4 + 0.1 M Na_2SO_4 ( ) and Au(1 1 1)/0.015 mM Ag_2SO_4 + 5 mM H_2SO_4 + 0.1 M Na_2SO_4 ( ) applying the routines 1 and 2 described in the inset, respectively. $|dE/dt| = 10\,mV\,s^{-1}$. The cyclic voltammogram for the system Ag(1 1 1)/Cd^{2+} ( ) is also included for comparison.

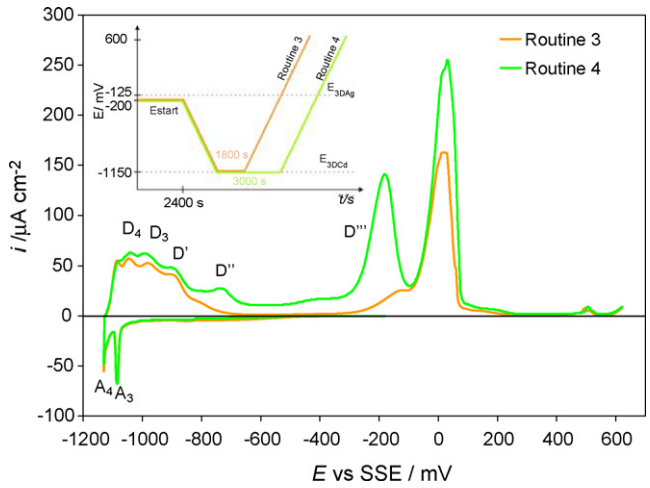

Fig. 7. Voltammetric adsorption/desorption behavior of the system Au(1 1 1)/Ag^+, Cd^{2+}, SO_4^{2-} after a potentiostatic experiment at $E_{start} = -200\,mV$ during $t_d = 2400\,s$ (routines 3 and 4), $|dE/dt| = 10\,mV\,s^{-1}$.

the 3D bulk deposition of the more noble metal very slowly under diffusion control [3,12,18]. As a consequence, the co-deposition of both metallic ions is very low, as was previously demonstrated [22]. Fig. 6 displays the corresponding voltammetric behavior. During the cathodic scan the characteristic peaks corresponding to the Cd UPD on Au(1 1 1) (cf. Fig. 1c) are not observed. In contrast, the voltammogram exhibits peaks related to the Cd UPD on Ag(1 1 1). This effect is an evidence that also in this case the Au(1 1 1) surface is completely screened by an epitaxially deposited thin Ag layer, formed during the polarization at E_{start}, on top of which the Cd UPD took place. However, the first peaks associated to the formation of a Cd expanded adlayer are absent and those related to the formation of a condensed phase are slightly displaced to more negative potentials, as was observed in the experiment described in Fig. 4. These results would indicate some inhibition for the Cd UPD onto the Au(1 1 1) substrate modified with Ag. During the anodic scan two peaks are recorded, which are coincident with the first two Cd desorption peaks observed in the system Ag(1 1 1)/Cd^{2+}. At more positive potentials other anodic peaks are recorded, which correspond to the stripping of the 3D Ag layer and the desorption of the UPD Ag adlayer, initially deposited on the Au(1 1 1) at E_{start}. From the corresponding charge of these peaks ($|\Delta q_{exp}| \approx 826\,\mu C\,cm^{-2}$) it could be concluded that ~3.7 Ag ML were deposited.

Fig. 6 also shows the anodic stripping curve obtained for the Au(1 1 1) in a solution containing only Ag^+ ions, following the polarization routine 2. In this blank experiment the corresponding Ag stripping charge was $|\Delta q_{exp}| \approx 815\,\mu C\,cm^{-2}$. In both experiments the shape of the Ag stripping curves is practically the same. Moreover, the difference between the Ag stripping charges is very low and could be ascribed to the additional Ag deposit produced during the scan up to −1150 mV in the case of the Cd^{2+} containing solution. Therefore, it can be concluded that the amount of Ag co-deposited with Cd, when both metallic ions are present, is very low.

To analyze the surface alloy formation process and/or co-deposition of Ag and Cd in this system, the polarization routines 3 and 4 were applied, which are schematized in the inset of Fig. 7. The routine 3 is similar to routine 1 (Fig. 6), but in this case the Au(1 1 1)/Ag modified substrate was maintained at $E = -1150\,mV$ ($\Delta E_{3DCd} = 0\,mV$) during a polarization time, $t_p = 1800\,s$, in order to allow the self-diffusion of the species if a surface alloy takes place. The subsequent anodic scan (Fig. 7) showed not only an increase in the charge corresponding to the peaks D_4 and D_3, but also the appearance of the peaks D' ($-950 \le E\,(mV) \le -850$), D'' ($-850 \le E\,(mV) \le -650$) and D''' ($-300 \le E\,(mV) \le -100$). The peaks D' and D'' were also observed in the experiment described in Fig. 5b, when the thin films were obtained from separated electrolytes. All these anodic peaks indicate the stripping of different surface alloy phases formed at very low underpotentials. The charge corresponding to the anodic peak related to the Ag dissolution was only slightly higher than that registered when the potential was continuously swept (routine 1).

Finally, the potential of the Au(1 1 1)/Ag modified substrate was maintained during $t_p = 3000\,s$ at $E = -1150\,mV$ ($\Delta E_{3DCd} = 0\,mV$) and subsequently polarized anodically according to the polarization routine 4 (inset of Fig. 7). In this case, the anodic peaks attributed to the dissolution of different surface alloy phases showed a significant charge increase (Fig. 7), especially that recorded in the potential range $-300 \le E\,(mV) \le -100$ (D''').

From the results shown above, although it was possible to prepare a Au(1 1 1)/Ag/Cd "sandwich" heterostructure, the formation of different alloy phases Ag–Cd or Au–Ag–Cd, originated by self-diffusion of the respective atoms, could be inferred. Moreover, though the experimental conditions tend to diminish the co-deposition effect, it cannot be totally neglected and some of the anodic peaks could be related to the stripping of Ag–Cd phases formed by this process.

In order to clarify this situation, the morphology changes of the Au(1 1 1) substrate during the formation and dissolution of the Au(1 1 1)/Ag/Cd heterostructure were followed by *in situ* STM. Fig. 8 shows the development of the Ag–Cd film onto Au(1 1 1) from the solution containing both Ag^+ and Cd^{2+} ions. In the potential range $100 \le E\,(mV) \le 550$, where the formation of an expanded Ag adlayer takes place [27], no changes of the surface topography were observed. A growth front at step edges appeared in the *in situ* STM image after stepping the potential to a value of $E = -200\,mV$ ($\eta_{3DAg} = -75\,mV$), which is more evident with the increase of the polarization time at a constant potential (Fig. 8a(1–3)). This effect continues until the Au surface is practically covered (Fig. 8a(4–7)), reaching a complete Ag ML onto the Au(1 1 1) surface (Fig. 8a(8)). The very low growth rate observed in the experiment can be attributed to the very low Ag^+ concentration present in the solution [12]. Nevertheless, some STM tip influence on this behavior could not be disregarded. The decrease of the Ag^+ concentration underneath the STM tip could be enhanced by the tip proximity. This effect can be related to both an electrostatic repulsion of Ag^+ by the positively charged tip and a reduced mass transport towards

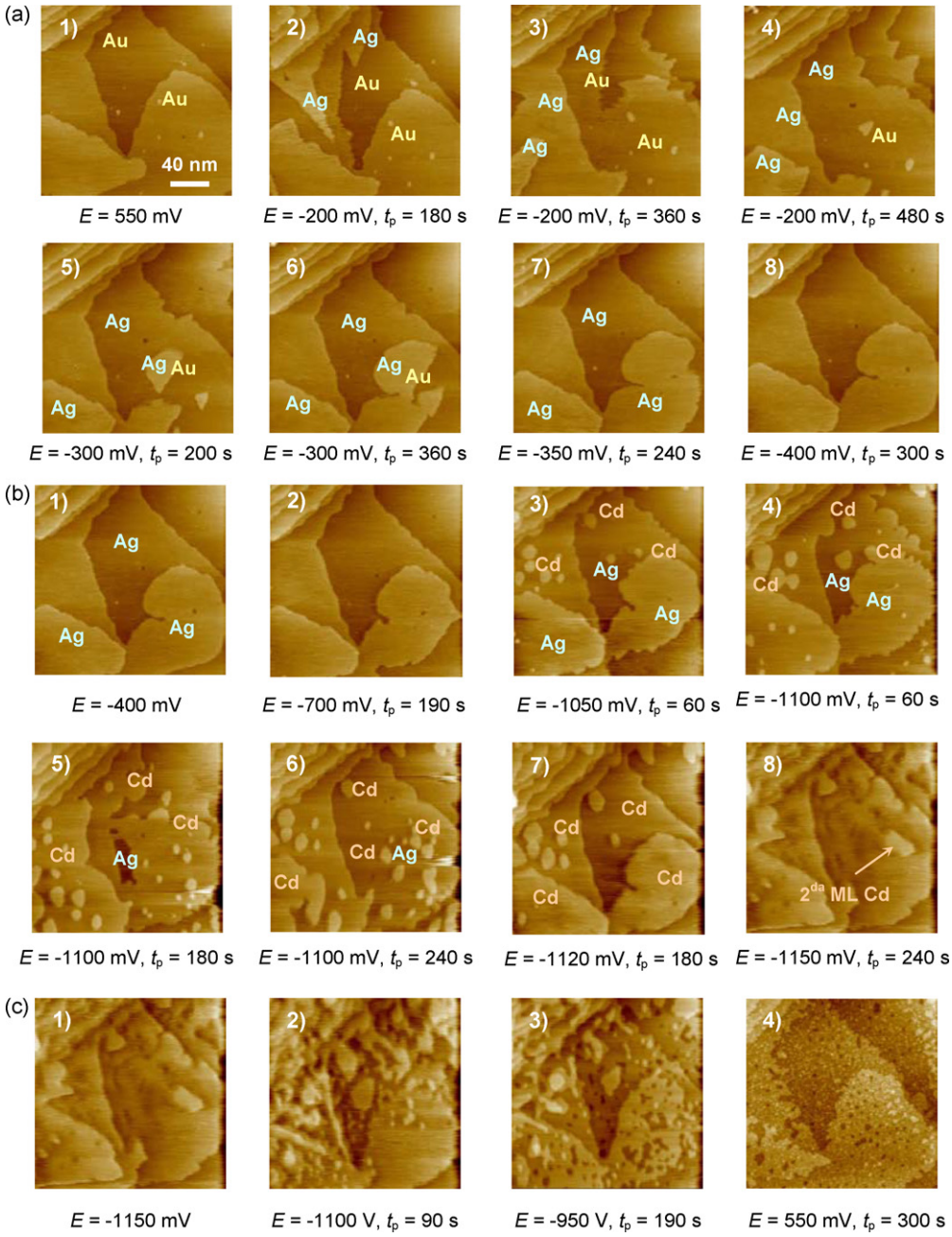

Fig. 8. *In situ* STM images obtained in the system Au(1 1 1)/0.015 mM Ag_2SO_4 + 1 mM $CdSO_4$ + 5 mM H_2SO_4 + 0.1 M Na_2SO_4. T = 298 K. (a) Formation of the Ag film, (b) deposition of the Cd film, (c) stripping of the heterostructure Au–Ag–Cd.

the metal surface underneath the tip due to the so-called shielding effect [33,34]. Afterwards, this Au(1 1 1)/1 Ag ML modified surface was polarized to more negative potentials in order to produce the Cd deposition (Fig. 8b). This process starts at $E \approx -750$ mV with the formation of a Cd expanded adlayer onto the Ag surface [22]. Nevertheless, in the present work the Cd deposition was evident at $E = -1050$ mV with the relatively fast growth of steps together with the nucleation of 2D islands (Fig. 8b(1–3)). This process is increased at a constant potential, originating the coalescence of the islands formed (Fig. 8b(4–6)).

At potentials, $E \approx -1120$ mV, very close to the E_{3DCd}, the initial image corresponding to the surface morphology of the Au(1 1 1)/1 Ag ML modified surface was reproduced (Fig. 8b(7)), i.e. it was formed a complete Cd ML on the Ag ML previously deposited on the Au(1 1 1) surface. Finally, the polarization at $E_{3DCd} = -1150$ mV during longer times produced new 2D Cd islands nucleated onto the monolayer recently formed in UPD, which corresponds to the beginning of a second Cd ML (Fig. 8b(8)). These results are in agreement with those reported for the binary system Ag(1 1 1)/Cd^{2+} [22].

The anodic stripping of this heterostructure was also followed by *in situ* STM (Fig. 8c). After the dissolution of the Cd and Ag deposits (Fig. 8c(1–3)) the original terraces of the Au(1 1 1) surface appeared, revealing many holes and little islands of monatomic height as shown in Fig. 8c(4) (cf. Fig. 8a(1)). These STM results demonstrated that during the cathodic sweep a Au(1 1 1)/1 Ag ML/1 Cd ML "sandwich" heterostructure was formed. Nevertheless, during this deposition process the intermixing of Cd and Ag atoms occurred, also affecting the first Au atomic layers. The last affirmation, supported by the appearance of many holes on the original gold terraces, can only be explained by considering a solid state diffusion process of Cd, Ag and Au atoms. This mechanism produces different Ag–Cd or Au–Ag–Cd alloy phases, which could be

responsible for the voltammetric response shown in Fig. 7. Consequently, further work using a powerful technique such us X-ray Photoelectron Spectroscopy (XPS), is required in order to determine the atomic distribution of the components of these surface alloys. This work is now in progress.

4. Conclusions

Ag/Cd ultrathin films on Au(1 1 1), were obtained by electrochemical deposition from separate electrolytes containing Ag^{+} and Cd^{2+} ions as well as from a multicomponent solution containing both ions. The polarization conditions were adjusted to produce, initially, a Ag film by OPD, and subsequently, a Cd ML by UPD onto this Ag film. The voltammetric behavior of the Cd UPD and the STM images indicated that the Au(1 1 1) substrate was totally screened by the ultrathin Ag layers initially formed, which were epitaxially oriented with respect to the Au(1 1 1) surface. Anodic stripping curves obtained after long time polarization experiments demonstrated that the formation of the Cd ML on this Ag layer was accompanied by a significant Ag–Cd surface alloying irrespective of the Ag film thickness. Additionally, *in situ* STM images obtained during the formation and the subsequent dissolution of a Au(1 1 1)/1 Ag ML/1 Cd ML modified surface in the multicomponent electrolyte, revealed a solid state diffusion process of Cd, Ag and Au atoms which can produce different Ag–Cd or Au–Ag–Cd alloy phases.

Acknowledgements

The authors wish to thank the Universidad Nacional del Sur (PGI 24/M110) and the Agencia de Promoción Científica (PICTO-UNS 2004 Cod. 614), Argentina, for financial support of this work. María Cecilia del Barrio acknowledges a fellowship granted by CONICET.

References

[1] D.M. Kolb, in: H. Gerischer, C. Tobias (Eds.), Advances in Electrochemistry and Electrochemical Engineering, vol. 11, Wiley, Germany, 1978, p. 125.
[2] R.R. Adzic, in: H. Gerischer, C. Tobias (Eds.), Advances in Electrochemistry and Electrochemical Engineering, vol. 13, Wiley, Germany, 1984, p. 159.
[3] E. Budevski, G. Staikov, W.J. Lorenz, Electrochemical Phase Formation and Growth. An Introduction to the Initial Stages of Metal Deposition, VCH Weinheim, 1996.
[4] E. Budevski, G. Staikov, W.J. Lorenz, Electrochim. Acta 45 (2000) 2559.
[5] M. Paunovic, M. Schlesinger, Fundamentals of Electrochemical Deposition, John Wiley & Sons, 2006.
[6] G. Staikov, A. Milchev, in: G. Staikov (Ed.), Electrocrystallization in Nanotechnology, Wiley–VCH Weinheim, 2007, p. 3.
[7] T.L. Wade, R. Vaidyanathan, U. Happek, J.L. Stickney, J. Electroanal. Chem. 500 (2001) 322.
[8] H. Siegenthaler, in: R. Wiesendanger, H.-J. Güntherodt (Eds.), Scanning Tunneling Microscopy II, Springer, 1995, p. 7.
[9] A.A. Gewirth, B.K. Niece, Chem. Rev. 97 (1997) 1129.
[10] S. Bharathi, V. Yegnaraman, G. Prabhakara Rao, Electrochim. Acta 36 (1991) 1291.
[11] J. Villegas, J.L. Stickney, J. Electrochem. Soc. 139 (1992) 686.
[12] H.-J. Pauling, K. Jüttner, Electrochim. Acta 37 (1992) 2237.
[13] H.-J. Pauling, G. Staikov, K. Jüttner, J. Electroanal. Chem. 376 (1994) 179.
[14] S.A. Abd El-Maksoud, S. Taguchi, T. Fukuda, A. Aramata, Electrochim. Acta 41 (1996) 1947.
[15] S.P.E. Smith, H.D. Abruña, J. Phys. Chem. B 103 (1999) 6744.
[16] S. Takami, G.K. Jennings, P.E. Laibinis, Langmuir 17 (2001) 441.
[17] S. Hwang, J. Lee, J. Kwak, J. Electroanal. Chem. 579 (2005) 143.
[18] W.J. Lorenz, G. Staikov, Surf. Sci. 335 (1995) 32.
[19] G. Staikov, K. Jüttner, W.J. Lorenz, E. Budevski, Electrochim. Acta 39 (1994) 1019.
[20] H.-J. Pauling, U. Schmidt, G. Staikov, K. Jüttner, W.J. Lorenz, E. Budevski, Proceedings of the Symposium on Electrochemically Deposited Thin Films vol. 93-26, The Electrochemical Society, Inc. Pennington, NJ. USA, 1993, p. 19.
[21] J.L. Stickney, in: A.J. Bard, I. Rubinstein (Eds.), Electroanalytical Chemistry, vol. 21, M. Deker, New York, 1999, p. 75.
[22] M.C. del Barrio, D.R. Salinas, S.G. García, Electrochem. Commun. 9 (2007) 1382.
[23] S.G. García, D.R. Salinas, G. Staikov, Surf. Sci. 576 (2005) 9.
[24] M.C. del Barrio, S.G. García, C.E. Mayer, D. Salinas, Surf. Interface Anal. 40 (2008) 22.
[25] S. Maupai, Y. Zhang, P. Schmuki, Surf. Sci. 527 (2003) L165.
[26] K. Engelsmann, W.J. Lorenz, E. Schmidt, J. Electroanal. Chem. 114 (1980) 1.
[27] S. García, D. Salinas, C. Mayer, E. Schmidt, G. Staikov, W.J. Lorenz, Electrochim. Acta 43 (1998) 3007.
[28] V. Rooryck, F. Reniers, C. Buess-Herman, G.A. Attard, X. Yang, J. Electroanal. Chem. 482 (2000) 93.
[29] M.J. Esplandiu, M.A. Schneeweiss, D.M. Kolb, Phys. Chem. Chem. Phys. 1 (1999) 4847.
[30] M.D. Lay, K. Varazo, N. Srisook, J.L. Stickney, J. Electroanal. Chem. 554 (2003) 221.
[31] H. Bort, K. Jüttner, W.J. Lorenz, G. Staikov, Electrochim. Acta 28 (1983) 993.
[32] R. Vidu, S. Hara, Surf. Sci. 452 (2000) 229.
[33] U. Stimming, R. Vogel, D.M. Kolb, T. Will, J. Power Sources 43 (1993) 169.
[34] S.G. García, D.R. Salinas, C.E. Mayer, W.J. Lorenz, G. Staikov, Electrochim. Acta 48 (2003) 1.